ment (*23*). Because, in the case of *P. abyssi*, eukaryotic-like replication proteins are used in a manner similar to that in Bacteria, the first possibility is unlikely. It remains to be established if similarities of archaeal and bacterial replication systems are a consequence of their common prokaryotic life-style (convergence) or if they are evolutionarily related (homologous). The latter hypothesis is supported by the observation that DnaA and Orc1/Cdc6 belong to the same protein superfamily (*24*), suggesting that all cellular replication initiation mechanisms originated in a DNA-based ancestor.

References and Notes

1. G. J. Olsen and C. R. Woese, *Cell* **89**, 991 (1997); D. R. Edgell and W. F. Doolittle, *Cell* **89**, 995 (1997).
2. R. Bernander, *Mol. Microbiol.* **29**, 955 (1998); I. K. Cann and Y. Ishino, *Genetics* **152**, 1249 (1999).
3. D. D. Leipe, L. Aravind, E. V. Koonin, *Nucleic Acids Res.* **27**, 3389 (1999).
4. I. K. Cann *et al.*, *J. Bacteriol.* **181**, 6591 (1999); Z. Kelman, S. Petrokovski, J. Hurwitz, *J. Biol. Chem.* **274**, 28751 (1999); G. Desogus, S. Onesti, P. Brick, P. Rossi, F. M. Pisani, *Nucleic Acids Res.* **27**, 4444 (1999); T. J. Kelly, P. Simancek, G. S. Brush, *Proc. Natl. Acad. Sci. U.S.A.* **95**, 14634 (1998).
5. J. R. Lobry, *Mol. Biol. Evol.* **13**, 660 (1996).
6. J. Mrazek and S. Karlin, *Proc. Natl. Acad. Sci. U.S.A.* **95**, 3720 (1998); S. Karlin, *Trends Microbiol.* **7**, 305 (1999).
7. A. Grigoriev, *Nucleic Acids Res.* **26**, 2286 (1998). In the case of *M. thermoautotrophicum*, one replication origin has been also predicted with an independent method [E. P. C. Rocha, A. Danchin, A. Viari, *Mol. Microbiol.* **32**, 11 (1999)].
8. P. Lopez, H. Myllykallio, H. Philippe, P. Forterre, *Mol. Microbiol.* **32**, 883 (1999).
9. The genome sequence of *P. abyssi* is available at www.genoscope.cns.fr/cgi-bin/Pab.cgi.
10. H. Myllykallio *et al.*, data not shown.
11. D. L. Maeder *et al.*, *Genetics* **152**, 1299 (1999).
12. Briefly, *P. abyssi* cultures were grown using enriched Vent Sulfothermophiles medium to an optical density at 600 nm (OD_{600}) = 0.12 and were treated with puromycin (200 μg/ml) for 110 min. The drug was removed by extensive washes with growth medium at 4°C. Treated cells were then reinoculated to OD_{600} = 0.10 in the presence of ^{14}C-labeled uracil (2 μCi/ml), and labeling was continued for indicated times (Fig. 2). Agarose plugs for CHEF analyses (6.5 V/cm, a linear pulse ramp of 3 to 17 s for 20 hours, 14°C) were prepared from 5-ml cultures by using a modification of standard protocols. Gels and filters (1 to 2 weeks of exposure to Storage Phosphor screens) were analyzed with a Storm imaging system (Molecular Dynamics, Sunnyvale, CA). Radioactivity of each Not I fragment was determined by using ImageQuant software and following the manufacturer's recommendations. To ensure that the results obtained were not an artifact of the puromycin treatment, the relative steady-state levels of Not I fragments were also investigated in untreated early exponential stage cultures. In this case, CHEF gels were stained with VistraGreen (Molecular Dynamics), a DNA-specific fluorescence dye, and were directly scanned with a blue fluorescence mode of a Storm system. Relative frequencies for fragments were obtained by dividing the amount of radioactivity/fluorescence of a given band by its size calculated on the basis of the determined genome sequence. All analyzed signals were within a linear range of a Storm system. The given values were normalized to the minimal value of one arbitrary unit and are averages of two independent measurements.
13. J. Leatherwood, *Curr. Opin. Cell Biol.* **10**, 742 (1998).
14. This region is interrupted by several stop codons in the three *Pyrococcus* genomes, indicating that it does not contain genes that could have been missed during the genome annotation.
15. The genome of *P. abyssi* contains 38 intergenic regions that are longer than 600 bp. When run through the BLAST program, only seven of these yield an expect score of $<1.0 \times 10^{-10}$ against the *P. horikoshii* genome, whereas the origin region gets an expect score of 1.0×10^{-33}. The use of the TBLASTX program indicates that the high scores of the remaining six intergenic regions might be due to some hard-to-identify open reading frames.
16. Available at www.sciencemag.org/feature/data/1048232.shl.
17. N. Ogasawara *et al.*, in *The Bacterial Chromosome*, K. Drlica and M. Riley, Eds. (American Society for Microbiology, Washington, DC, 1990), pp. 287–299.
18. J. M. Louarn, J. Louarn, V. Francoise, J. Patte, *J. Bacteriol.* **173**, 5097 (1991); H. Bierne and B. Michel, *Mol. Microbiol.* **13**, 17 (1994).
19. G. Blakely *et al.*, *Cell* **75**, 351 (1993).
20. The MCM protein of *M. thermoautotrophicum* acts as an adenosine triphosphate–dependent 3′–5′ DNA helicase [Z. Kelman, J. K. Lee, J. Hurwitz, *Proc. Natl. Acad. Sci. U.S.A.* **96**, 14783 (1999); J. P. J Chong, M. K. Hayashi, M. N. Simon, R.-M. Xu, B. Stillman, *Proc. Natl. Acad. Sci. U.S.A.* **97**, 1530 (2000).
21. B. Stillman, in *DNA Replication in Eukaryotic Cells*, M. DePamphilis, Ed. (Cold Spring Harbor Laboratory Press, Cold Spring Harbor, NY, 1996), pp. 435–460; A. Dingwall and L. Shapiro, *Proc. Natl. Acad. Sci. U.S.A.* **86**, 119 (1989).
22. P. Lopez and H. Philippe, unpublished data.
23. P. Forterre, *Mol. Microbiol.* **33**, 457 (1999).
24. A. F. Neuwald, L. Aravind, J. L. Spounge, E. V. Koonin, *Genome Res.* **9**, 27 (1999).

25. This work was supported by research grants from the European Union (BIO-CT 96-0488) and the Association de Recherche contre le Cancer. H.M. acknowledges financial support from the European Union and thanks U. Liebl for helpful discussions. We thank J. Weissenbach and his staff for sequencing the complete genome of *P. abyssi*.

27 December 1999; accepted 19 April 2000

Requirement of Mis6 Centromere Connector for Localizing a CENP-A–Like Protein in Fission Yeast

Kohta Takahashi,[1,2,3] Ee Sin Chen,[1,2] Mitsuhiro Yanagida[1,2,3]*

Mammalian kinetochores contain the centromere-specific histone H3 variant CENP-A, whose incorporation into limited chromosomal regions may be important for centromere function and chromosome segregation during mitosis. However, regulation of CENP-A localization and its role have not been clear. Here we report that the fission yeast homolog SpCENP-A is essential for establishing centromere chromatin associated with equal chromosome segregation. SpCENP-A binding to the nonrepetitious inner centromeres depended on Mis6, an essential centromere connector protein acting during G_1-S phase of the cell cycle. Mis6 is likely required for recruiting SpCENP-A to form proper connection of sister centromeres.

The kinetochore is a chromosomal architecture serving as the attachment site for spindle microtubules and is crucial for directing faithful chromosome segregation during mitosis (*1*). Because mutations in Mis6 and Mis12, two essential centromere proteins of the fission yeast *Schizosaccharomyces pombe*, disrupt centromere chromatin and cause high frequencies of missegregation (*2*, *3*), it is thought that the composition and/or modifications of the nucleosomes underlying centromere chromatin might be altered. Both mammalian CENP-A and its budding yeast homolog Cse4 function as essential histone-like components of the centromere nucleosomes (*4*, *5*).

To assess the possible role of CENP-A in centromere integrity and function, the gene encoding the CENP-A homolog in *S. pombe* was identified (*6*). Sequencing revealed a putative histone H3 variant clone [designated SpCENP-A; the formal gene name is *cnp1*$^+$ (centromere protein 1)] (Fig. 1A) encoding a polypeptide of 120 amino acids (*6*) with 57, 53, and 48% identity to the fission yeast histone H3, the budding yeast Cse4, and human CENP-A, respectively.

To examine intracellular localization of SpCENP-A, we constructed a fusion gene comprised of SpCENP-A with its native promoter and green fluorescent protein (GFP) that we confirmed to be functional (*7*) and integrated into the genome. SpCENP-A–GFP was seen as single dots near the nuclear periphery in interphase cells (Fig. 1B, top row). Two or three dots were observed in prometaphase or metaphase cells (Fig. 1B, rows 2 and 3) and one dot was present per daughter nucleus in anaphase cells (Fig. 1B, rows 4 and 5). In mitotically arrested β-tubulin mutant *nda3-311* (*8*), a single centromere-like locus of GFP signal was seen on each of

[1]CREST Research Project, Japan Science and Technology Corporation. [2]Department of Biophysics, Graduate School of Science, [3]Department of Gene Mechanisms, Graduate School of Biostudies, Kyoto University, Kitashirakawa-Oiwakecho, Sakyo-ku, Kyoto 606-8502, Japan.

*To whom correspondence should be addressed. E-mail: yanagida@kozo.biophys.kyoto-u.ac.jp

three condensed chromosomes (Fig. 1B, bottom row). Hence, SpCENP-A–GFP followed the same cell cycle dynamics as that reported for centromeres (*9*).

Fission yeast centromeres are several hundred times as large as those of budding yeast and contain repetitive DNA sequences like the centromeres of higher organisms (*1*). The three centromere DNA sequences (*cen1*, *-2*, and *-3*) vary in size (30 to 120 kb), but are organized in a similar fashion in all chromosomes (*10*) (Fig. 1C, upper diagram). The inner centromere regions (*cnt* and *imr*) are nonrepetitive and are functionally essential, whereas the outer centromere regions (*otr*) consist of repetitive motifs. With the use of chromatin immunoprecipitation (CHIP) analysis (*2*), we examined whether centromeric DNAs coimmunoprecipitated with SpCENP-A that is epitope-tagged with hemagglutinin antigen (HA) (*7*). Polymerase chain reaction (PCR) primers corresponding to the centromere (*cnt*, *imr*, *otr*) and the pericentric region (*lys1*) were used for identifying coimmunoprecipitated DNA sequences (Fig. 1C, lower). Amplified PCR products were detected for *cnt* and *imr* but not for *otr* and *lys1*, indicating that SpCENP-A is predominantly localized to the essential nonrepetitive inner centromeres. The inner centromere DNA has been shown to contain specialized chromatin that gives the smear micrococcal nuclease (MNase) digestion pattern (*10*).

To address whether SpCENP-A is required for establishing this inner centromere chromatin structure, we used chromatin fractions of SpCENP-A–null cells (*11*) for MNase digestion after germination (*12*). In wild-type controls, the digestion patterns of the inner centromere DNA (*cnt* and *imr*) were smeared, whereas the outer repetitive (*otr*) regions showed a regular nucleosomal pattern (Fig. 2A, wt). In contrast, the smeared pattern was abolished in disruptant (null), indicating that SpCENP-A is required for formation of inner centromere-specific chromatin.

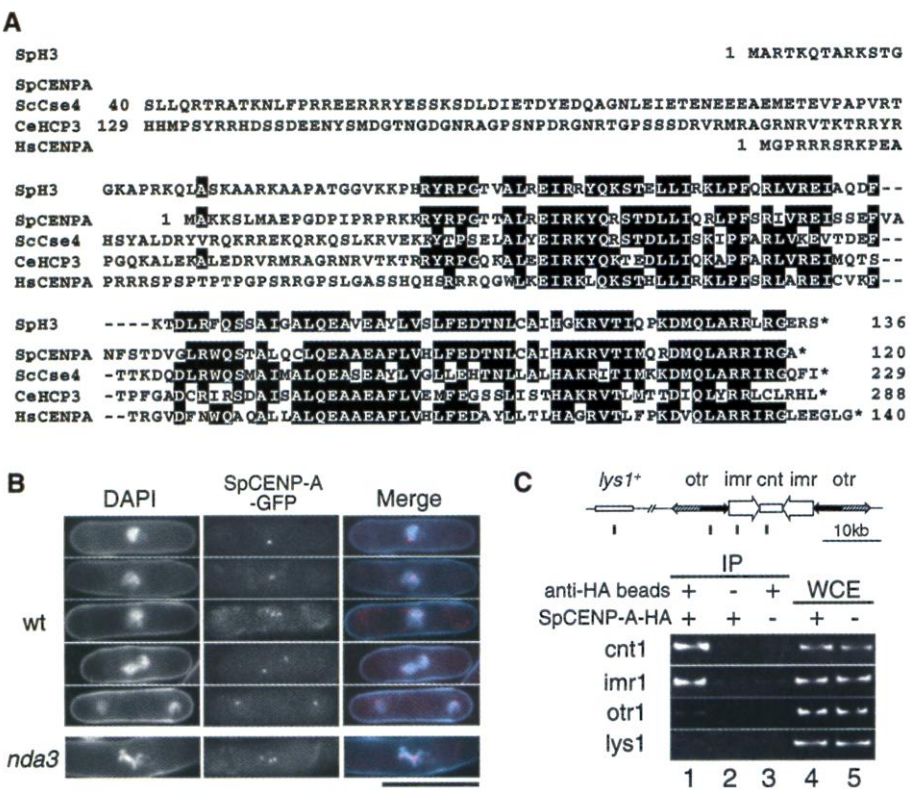

Fig. 1. SpCENP-A is an inner centromere-specific histone H3 variant. (**A**) Sequence alignment of SpCENP-A with *S. pombe* histone H3 (*20*), *S. cerevisiae* Cse4 (*15*), *C. elegans* HCP-3 (*14*), and *Homo sapiens* CENP-A (*4*). Accession number of SpCENP-A in DNA Databank of Japan (DDBJ) database, AB041724 (*23*). (**B**) Cellular localization of SpCENP-A during the cell cycle. Wild-type and the prophase-arrested *nda3-311* cells carrying the integrated SpCENP-A–GFP gene. DAPI (4′6-diamidino-2-phenylindole) was used to stain DNA. Red, SpCENP-A–GFP; blue, DAPI. Bar, 10 μm. (**C**) SpCENP-A–HA expressed in wild-type cells was immunoprecipitated (IP) for CHIP analysis (*2*) with antibody to HA (anti-HA) conjugated to beads. Coimmunoprecipitated DNA was amplified by PCR with four different primers (their location shown as vertical lines in a schematic drawing for *cen1*). Approximately the same amount of PCR product was obtained from the whole cell extracts (WCE) of cells with and without SpCENP-A–HA (lanes 4 and 5). Lanes 2 and 3 are the control lanes either using beads alone or the extract without SpCENP-A–HA, respectively. Quantification of the band intensity after background titration revealed that the amount of the PCR products of *otr* and *lys1* were less than 5% of those of *cnt* and *imr*.

SpCENP-A–null cells produce unequal-sized nuclei during mitosis, increasing in frequency after one or two cycles of cell division and becoming very high (76 to 88% in cells containing two nuclei) after 14 to 20 hours (Fig. 2B) (*12*). Cytokinesis occurred after unequal nuclear division, leading to aneuploidy. To assess the behavior of centromeres during mitosis, we used a cen1-GFP probe (*9*) to visualize centromeric DNA in SpCENP-A–null cells. Under the culture condition used, 73% of the binucleate cells contained asymmetric nuclei, whereas 18% had two discrete cen1-GFP signals within one nucleus (Fig. 2C, top). The remaining binucleate cells had normally distributed cen1-GFP signals, but most nuclei were unequal in size, indicating missegregation for other chromosomes (Fig. 2C, bottom). A temperature-sensitive (*ts*) allele *cnp1-1* (*13*) exhibited a phenotype at the restrictive temperature (36°C) identical to that of the SpCENP-A–null mutant, with decreased viability after unequal mitotic segregation (Fig. 2D). This type of missegregation was also observed in *Caenorhabditis elegans* embryos with the reduced level of CENP-A–like protein (*14*). In SpCENP-A–deficient cells, mitotic progression was not obviously delayed and "streaked" or "lagging" chromosomes were rarely observed. Thus, sister chromatids were separated and moved to the poles, but the fidelity of equal segregation was greatly reduced. This is in contrast to the mitotic arrest phenotype described for *ts* mutants and null mutants of *Saccharomyces cerevisiae CSE4* (*5*, *15*).

Disruption of the centromere chromatin in SpCENP-A–deficient cells could be due to chromosome loss (rather than the loss of a specific SpCENP-A function) during unequal segregation, which in turn might eliminate factors essential for making the centromere chromatin. To examine this possibility, we performed a MNase digestion experiment with a synchronous G_1 cell population (Fig. 2E). DNA replication took place 3 to 4 hours after release. The smear patterns of *imr* were observed in both G_1-arrested and exponentially growing wild-type cells (wt and *imr* at 0 and 10 hours). In contrast, the smear pattern in centromere chromatin of SpCENP-A *ts* mutant was already partially reduced at 20°C and clearly lost at 6 hours in 36°C (*ts* mutant and *imr* at 0 and 6 hours), whereas cell viability still remained high and unequal segregation was not yet observed (2%) at 6 hours. In the *ts* mutant, the frequency of missegregation increased only after 8 hours (27%) and became prominent after 10 hours (64%) at 36°C, resulting in the decrease of cell viability. Thus, disruption of the centromere chromatin occurred before missegregation in SpCENP-A–deficient cells. Formation of this chromatin might be prerequisite for equal segregation during subsequent mitosis.

Mutations of Mis6 and Mis12, inner centromere proteins of *S. pombe*, cause premature separation of sister centromeres at metaphase and act during the G_1-S and previous M phases, respectively (*2*, *3*). Therefore, both proteins are implicated in the formation of a proper connection between sister centromeres. Because the phenotypes (e.g., disruption of centromere chromatin and unequal chromosome segregation) of null and *ts* mutants of SpCENP-A resemble those of *mis6* and *mis12* mutants (*2*, *3*), we addressed whether Mis6 and/or Mis12 might be involved in the association of SpCENP-A with centromeres. The expression of the integrated SpCENP-A–GFP gene in the genetic background of these *ts* mutants was examined at 20° and 36°C (Fig. 3A). In *mis6-302* at 20°C, SpCENP-A–GFP colocalized with the centromeres throughout the cell cycle but became dispersed at 36°C, fading out from the centromeres before chromosome missegregation occurred. In *mis12-537* mutant cells, however, SpCENP-A–GFP signals remained colocalized with the centromeres even after 6 hours at 36°C. The general sister chromatid cohesion molecules Mis4 (an adherin, similar to *S. cerevisiae* Scc2) (*16*) and Rad21 (a cohesin component, similar to Scc1) (*17*) were not required for SpCENP-A localization (*18*). Centromeric localization of Mis6-GFP or Mis12-GFP was not affected at 36°C in SpCENP-A *ts* mutant cells (*18*). Immunoblotting showed equal expression of SpCENP-A–GFP in *mis6-302*, *mis12-537*, and wild-type cells at 36°C (Fig. 3B), indicating that the fading of GFP signals in *mis6-302* was due to dispersion rather than proteolysis of SpCENP-A–GFP.

CHIP analysis demonstrated that SpCENP-A binding to the nonrepetitious inner centromeres depended on the presence of Mis6 (Fig. 3C). SpCENP-A binding to *cnt* and *imr* was reduced for 6 hours at 36°C in *mis6* cells

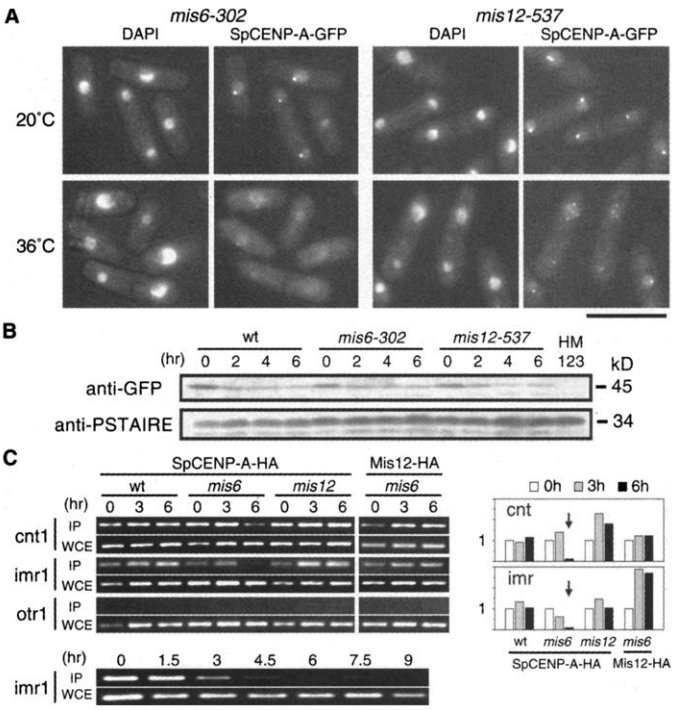

Fig. 3. Centromeric localization of SpCENP-A depends on Mis6. (**A**) Localization of SpCENP-A–GFP in the genetic background of *mis6-302* and *mis12-537* cultured in EMM2 medium at 20° or 36°C for 6 hours. Bar, 10 μm. (**B**) The SpCENP-A–GFP levels of the integrants cultured in EMM2 at 20° or 36°C for 2, 4, and 6 hours were determined by immunoblotting with antibodies to GFP (anti-GFP). The amount of Cdc2 [antibody to PSTAIRE (anti-PSTAIRE)] was used as a positive control for proper loading. HM123, a nonintegrated wild-type strain, was used as a negative control. (**C**) SpCENP-A–HA or Mis12-HA integrants in the genetic background of wild-type, *mis6-302*, and *mis12-537* were cultured in yeast extract, peptone, and dextrose (YPD) medium at 20° or 36°C, and were used for CHIP analysis (*2*). *cnt*, *imr*, and *otr* were the primers used. The amplified PCR products from immunoprecipitates (IP) and the WCE are shown. Band intensity of the PCR products was quantitated with respect to value of 0 hour in each group (e.g., for wt and SpCENP-A–HA, after the intensity of the IP was divided by that of the WCE, the value at 0 hour was normalized to 1 and the values at 3 and 6 hours were calculated proportionally). Shown at bottom is the CHIP analysis of a SpCENP-A–HA integrant in *mis6-302* using *imr* primers, showing a reduction in SpCENP-A binding at shorter time intervals.

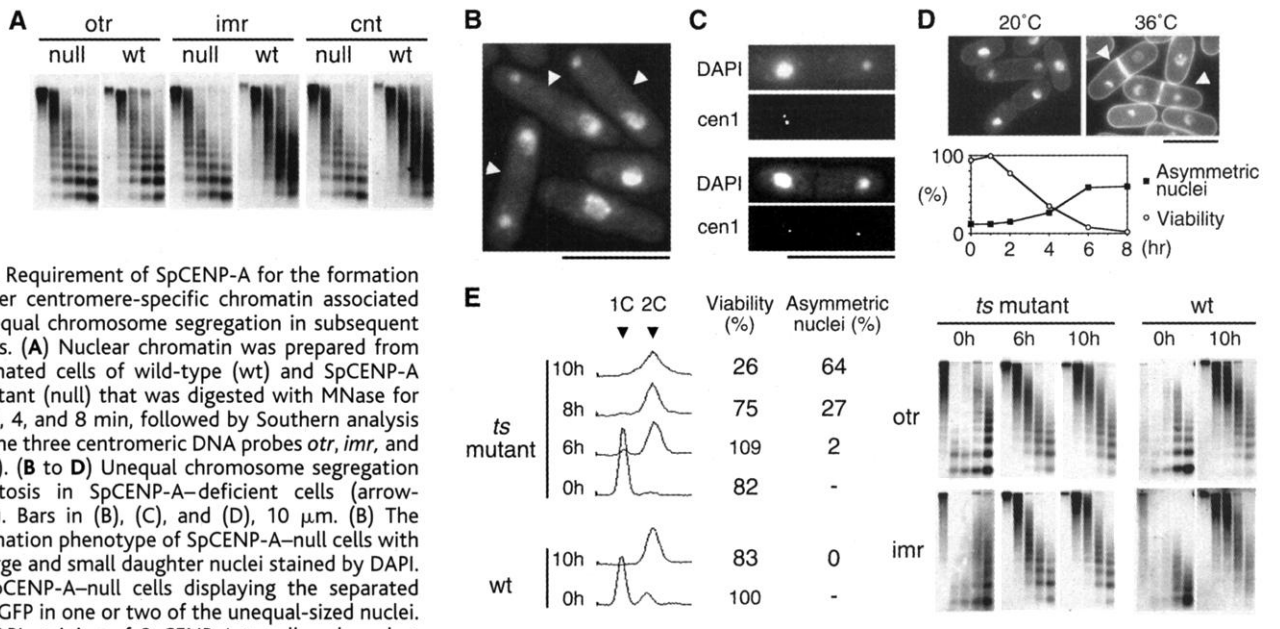

Fig. 2. Requirement of SpCENP-A for the formation of inner centromere-specific chromatin associated with equal chromosome segregation in subsequent mitosis. (**A**) Nuclear chromatin was prepared from germinated cells of wild-type (wt) and SpCENP-A disruptant (null) that was digested with MNase for 0, 1, 2, 4, and 8 min, followed by Southern analysis with the three centromeric DNA probes *otr*, *imr*, and *cnt* (*2*). (**B** to **D**) Unequal chromosome segregation in mitosis in SpCENP-A–deficient cells (arrowheads). Bars in (B), (C), and (D), 10 μm. (B) The germination phenotype of SpCENP-A–null cells with the large and small daughter nuclei stained by DAPI. (C) SpCENP-A–null cells displaying the separated Cen1-GFP in one or two of the unequal-sized nuclei. (D) DAPI staining of SpCENP-A *ts* cells cultured at 20° or 36°C for 6 hours (upper). Cell viability and frequency of binucleate cells with asymmetric nuclei at 36°C (lower). (**E**) The disruption of the inner centromere chromatin before unequal chromosome segregation in SpCENP-A *ts* cells (left). Wild-type and SpCENP-A *ts* cells in G_1 phase were prepared by nitrogen starvation at 20°C and were synchronously released at 36°C. Shown (right) are the DNA contents estimated by flow cytometry, cell viability, frequency of binucleate cells with asymmetric nuclei, and the MNase digestion experiment with *otr* and *imr* probes.

(less than 10% with respect to the value at 20°C) (Fig. 3C, right, arrow) but not in wild-type or *mis12* cells. The centromere binding of Mis12, however, was not reduced in *mis6* cells (see rightmost lane, Mis12-HA at 6 hours). A detailed time-course analysis confirmed the reduction in SpCENP-A binding to the inner centromere in *mis6* cells (Fig. 3C, bottom). These results support the cytological data, showing that Mis6 is required for association of SpCENP-A with the inner centromere chromatin.

Uncoupling of CENP-A expression from normal histone expression was proposed to be an important component for the CENP-A targeting mechanism (*19*). Transcriptional timing of SpCENP-A mRNA and regular histone mRNA was assessed for a synchronized cell culture (Fig. 4A). The amount of SpCENP-A mRNA was maximal at 30 to 45 min before the peak of the septation index (the greatest percentage of cells with the septum) and preceded maximal amount of histone H3 mRNA, which peaked at the onset of S phase (*20*). This indicated that SpCENP-A transcription occurred from the late M to G_1-S phase. Mammalian CENP-A mRNA peaked later than the S phase, as the timing of centromere DNA replication was also late (*19*). Timing of centromere DNA replication in *S. pombe* is unknown, but it might be early in the S phase as it is in budding yeast.

Because maximum levels of SpCENP-A mRNA were observed just before the G_1-S boundary when Mis6 functions (Fig. 4A) (*2*), we examined the localization of de novo synthesized SpCENP-A protein in Mis6-deficient cells. A SpCENP-A–GFP fusion gene under the control of an inducible promoter *nmt1* (*21*) was integrated at the *lys1* loci of wild-type, *mis6-302*, or *mis12-537* cells. Upon the removal of thiamine from the culture medium, 16 to 18 hours incubation at 20°C is required for induction of SpCENP-A–GFP in these strains. Just before the induction of SpCENPA-A–GFP (16 hours, 20°C), wild-type, *mis6* and *mis12* mutants were shifted to 36°C to see if newly synthesized SpCENP-A–GFP localized to centromeres. In all the strains examined, GFP signals were detected in 3 to 5% of cells at 2 hours and were observed in more than 90% of cells cultured at 4 hours at 36°C. In both wild-type and *mis12* cells, the induced signals accumulated into a single dot near the nuclear periphery (Fig. 4B). The induced GFP signals were incorporated into the centromere-like dots in *mis12* cells with typical unequal-sized nuclei for 8 hours at 36°C. In contrast, dispersed nuclear signals were observed that did not associate with dot-like structures in more than 80% of the *mis6-302* cells at 36°C. This mislocalization occurred at 36°C but not at 20°C, suggesting that Mis6 protein recruits SpCENP-A onto the centromeres.

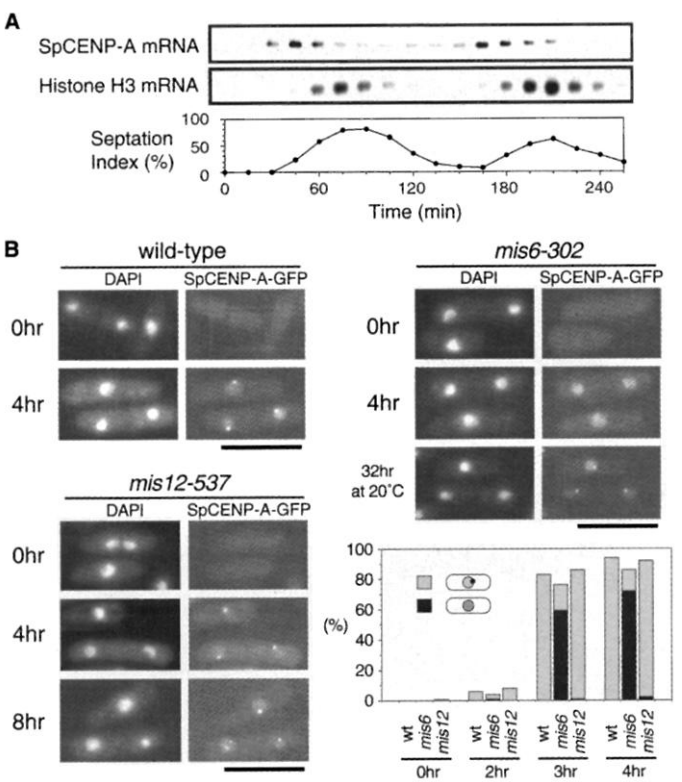

Fig. 4. Association of newly synthesized SpCENP-A onto centromeres requires Mis6, which acts during G_1-S phase. (**A**) The level of SpCENPA mRNA peaked just before G_1-S phase. SpCENP-A and histone H3.1 mRNA levels in synchronized cell cultures were monitored by Northern analysis (*24*). Frequencies of cells with septation are shown. (**B**) Localization of newly synthesized SpCENP-A–GFP under the control of *nmt1* promoter in wild-type, *mis12-537*, and *mis6-302* cells. Shown are cells cultured for 16 hours after the removal of thiamine in EMM2 at 20°C and subsequently cultured for 0, 4, and 8 hours after temperature shift to 36°C in each strain, and *mis6-302* cells cultured for 32 hours at 20°C (four rounds of division, as doubling time at 20°C is about 8 hours). Removal of thiamine from the culture medium activates the *nmt1* promoter (*21*). Bar, 10 μm. Lower right, frequencies of GFP-positive cells with (gray bar) and without (black bar) centromere-like signals in the nucleus.

This study shows that SpCENP-A is required for equal sister chromatid segregation and that its localization to the inner centromeres requires functional Mis6 possibly at the G_1-S boundary for forming inner centromere-specific chromatin. SpCENP-A and Mis6 are not sufficient for establishment of this chromatin, as Mis12 is also needed, presumably in a different timing (*3*). Incorporation at proper timing of newly synthesized SpCENP-A through Mis6 may be required to confer the bioriented connection of the sister centromeres after replication. This model would explain the phenotype of *mis6* mutant cells; inactivation from G_1 to M, but not from S to M, results in subsequent unequal mitosis (*2*). Mis6 may function as a loading chaperone of SpCENP-A, similar to CAF1 for histone H3 and H4 (*22*). Alternatively, Mis6 may directly bind to the centromeric DNA to induce a higher-order configuration and/or modification that might be required for SpCENP-A loading. In humans, a protein similar to Mis6 exists [hLRPR1 has 27% identity (*2*)], though its functions remain to be investigated.

References and Notes

1. G. H. Karpen and R. C. Allshire, *Trends Genet.* **13**, 489 (1997).
2. S. Saitoh, K. Takahashi, M. Yanagida, *Cell* **90**, 131 (1997).
3. G. Goshima, S. Saitoh, M. Yanagida, *Genes Dev.* **13**, 1664 (1999).
4. K. F. Sullivan, M. Hechenberger, K. Masri, *J. Cell Biol.* **127**, 581 (1994).
5. P. B. Meluh, P. Yang, L. Glowczewski, D. Koshland, M. M. Smith, *Cell* **94**, 607 (1998).
6. The CENP-A homolog gene in *S. pombe* was isolated by degenerate PCR amplification method with a genomic DNA library. Three conserved amino acid sequences in CENP-A, ALQEA(A/S)EA, EA(A/S)EA(F/Y)LV, and QLARR(I/L)RG (*23*), were used to synthesize the primers [5′-GCICT(A/G)CA(A/G)GA(A/G)GCN(T/G)(C/G)(T/C)GA(A/G)GC-3′, 5′-CC(T/G)CGIAT(T/C)CG(T/C)CGNGCNA(G/A)(T/C)TG-3′, and 5′-GA(A/G)GCI(T/G)(C/G)(T/C)GA(A/G)GCN(T/C)TNGT-3′, respectively (I, inosine; N, any)]. An amplified product revealed the CENP-A–like sequence with a high homology, but was not identical to the known fission yeast histone H3 genes. A part of the sequence (5′-CTACACGAGTGACGATTATGCAACGA-3′) was used for screening the genomic DNA clone containing the full-length coding region. Clones with the identical amino acid sequence determined by PCR were obtained by colony hybridization from a *S. pombe* genomic DNA library.
7. Integration plasmids containing the SpCENP-A gene ligated in-frame at the COOH-terminus with S65T-GFP (*3*) or triple tandem HA epitope (*2*) were integrated at the *lys1* locus of wild-type or SpCENP-A–null (*11*) cells. Both SpCENP-A–HA and SpCENP-A–GFP integrants in the null mutant background formed colonies, indicating that the tagged genes were functional. Immunoblot of SpCENP-A–HA integrant cell extracts by antibody to HA produced an expected 25-kD band.
8. Y. Hiraoka, T. Toda, M. Yanagida, *Cell* **39**, 349 (1984).
9. K. Nabeshima *et al.*, *Mol. Biol. Cell* **11**, 3211 (1998).
10. K. Takahashi *et al.*, *Mol. Biol. Cell* **3**, 819 (1992).
11. A linear DNA fragment carrying SpCENP-A disrupted by insertion of the *S. pombe ura4*$^+$ gene at the Eco RV sites in the coding region was introduced into Ura$^-$ diploid by transformation. Tetrad analysis of spores derived from Ura$^+$ heterozygous diploids showed that SpCENP-A was essential for viability.

12. Spores from wild-type or Ura$^+$ heterozygous diploid (*11*) were germinated in EMM2 at 33°C for 16 hours with and without uracil. Disruptant spores carrying the integrated *ura4*$^+$ gene could germinate in the absence of uracil. MNase digestion was performed as described (*2*).
13. A L87Q mutation similar to *cse4-103* was introduced into the SpCENP-A gene with the native promoter. The resultant *cnp1-1* mutant gene was integrated at the *lys1* locus of SpCENP-A–null strain.
14. B. J. Buchwitz, K. Ahmad, L. L. Moore, M. B. Roth, S. Henikoff, *Nature* **401**, 547 (1999).
15. S. Stoler, K. C. Keith, K. E. Curnick, M. Fitzgerald-Hayes, *Genes Dev.* **9**, 573 (1995).
16. K. Furuya, K. Takahashi, M. Yanagida, *Genes Dev.* **12**, 3408 (1998).
17. K. Tatebayashi, J. Kato, H. Ikeda, *Genetics* **148**, 49 (1998).
18. K. Takahashi, E. S. Chen, M. Yanagida, data not shown.
19. R. D. Shelby, O. Vafa, K. F. Sullivan, *J. Cell Biol.* **136**, 501 (1997).
20. S. Matsumoto and M. Yanagida, *EMBO J.* **4**, 3531 (1985).
21. K. Maundrell, *Gene* **123**, 127 (1993).
22. C. R. Adams and R. T. Kamakaka, *Curr. Opin. Genet. Dev.* **9**, 185 (1999).
23. Single-letter abbreviations for the amino acid residues are as follows: A, Ala; C, Cys; D, Asp; E, Glu; F, Phe; G, Gly; H, His; I, Ile; K, Lys; L, Leu; M, Met; N, Asn; P, Pro; Q, Gln; R, Arg; S, Ser; T, Thr; V, Val; W, Trp; and Y, Tyr.
24. *cdc25-22 ts* mutant cells [P. A. Fantes, *Nature* **279**, 428 (1979)] were shifted to 36°C for the arrest in G_2. Cells were synchronously released into mitosis by the shift to 26°C.
25. We thank M. M. Smith for *cse4-103* mutant and A. M. Carr for the gift of the *S. pombe* genomic DNA library. The present study was supported by the CREST research project of Japan Science and Technology Corporation.

25 February 2000; accepted 24 April 2000

Role of the Guanosine Triphosphatase Rac2 in T Helper 1 Cell Differentiation

Baiyong Li,[1,2]*† Hong Yu,[1,2]† Wei-ping Zheng,[1]‡ Reinhard Voll,[1,2]§ Songqing Na,[1]‖ Andrew W. Roberts,[3]¶ David A. Williams,[3] Roger J. Davis,[4] Sankar Ghosh,[1,2,5] Richard A. Flavell[1,2]#

T helper 1 (T_H1) cells mediate cellular immunity, whereas T_H2 cells potentiate antiparasite and humoral immunity. We used a complementary DNA subtraction method, representational display analysis, to show that the small guanosine triphosphatase Rac2 is expressed selectively in murine T_H1 cells. Rac induces the interferon-γ (IFN-γ) promoter through cooperative activation of the nuclear factor kappa B and p38 mitogen-activated protein kinase pathways. Tetracycline-regulated transgenic mice expressing constitutively active Rac2 in T cells exhibited enhanced IFN-γ production. Dominant-negative Rac inhibited IFN-γ production in murine T cells. Moreover, T cells from Rac2$^{-/-}$ mice showed decreased IFN-γ production under T_H1 conditions in vitro. Thus, Rac2 activates T_H1-specific signaling and IFN-γ gene expression.

T_H1 and T_H2 cells can be differentiated in vitro from common naïve precursor T cells during the course of a few days (*1*). During this time period, T_H1 or T_H2 regulatory proteins specific to each lineage are induced that are likely to play key roles in the differentiation process. To search for genes differentially expressed in T_H1 or T_H2 cells, we performed RDA (representational display analysis) (*2*) using in vitro–differentiated T_H1 and T_H2 cells. Using this procedure, we identified the transcription factor GATA3 as a T_H2-specific gene and a key regulator of T_H2 differentiation (*3*). Here we show that the small guanosine 5′-triphosphate (GTP)–binding protein Rac2 is a T_H1-specific gene that plays a central role in T_H1 development. A T_H1 probe generated after three rounds of RDA subtraction with primary T_H1 and T_H2 cDNA was used to screen a T_H1 cDNA library. Rac 2 was one of the genes identified. To confirm this result, we examined the expression level of Rac2 in day 4 T_H1 and T_H2 cells. A highly enriched Rac2 mRNA representation was found in primary T_H1 cells (Fig. 1A) while, as expected, GATA3 showed enrichment in T_H2 cells.

Rac has been shown to activate both JNK, p38, and NF-κB pathways (*4*–*6*) in various cell types. Moreover, JNK and p38 are selectively activated in T_H1 effector cells (*7*, *8*). This suggested that the elevated level of Rac2 might be the cause of the selective activation of these pathways. Consistent with these observations, constitutively active Rac2 (L61, GTP-bound) activated JNK and p38 pathways and NFκB in Jurkat cells, as shown by both direct measurement of JNK and p38 kinase activity (Fig. 1B) and AP1-luciferase (*9*), Chop-luciferase (*10*), and κB-luciferase (*11*) reporter gene activation (Fig. 1C), while having no effect on a reporter construct bearing binding sites for the ets family of transcription factors. A similar result was observed with Rac1L61 (*12*).

We first examined whether Rac2 plays a role in T_H1 cytokine gene expression. Constitutively active Rac2 cotransfected into Jurkat cells with an interferon-γ (IFN-γ) promoter reporter plasmid (*13*) induced a six- to sevenfold activation of the IFN-γ promoter, whereas CDC42L61 did not (Fig. 2A). To determine whether Rac2L61 activates IFN-γ expression in T cell clones, we cotransfected IFN-γ promoter reporter and the expression vector for Rac2L61 into the T_H1 clone AE7 (*14*) and the T_H2 clone D10 (*15*). Although Rac2L61 strongly activated the IFN-γ promoter in AE7 cells, it failed to activate the IFN-γ promoter in D10 cells (Fig. 2B).

To examine which of these signaling pathways—JNK, p38, or NF-κB–is required for Rac-mediated IFN-γ activation, we blocked each pathway with specific inhibitors. Whereas dominant-negative JNK1 or the ERK inhibitor PD98059 has no effect on RacL61-induced IFN-γ promoter activation, both the NF-κB super repressor (*16*) and the p38 inhibitor SB203580 inhibited this activation completely (Fig. 2C). We next examined whether any of these pathways was sufficient for Rac-mediated IFN-γ activation. Whereas activation of the JNK pathway with MKK7 and JNK1 (*17*), the p38 pathway with MKK6glu (*18*), or NF-κB with a constitutively active form of IKKβ (*19*) alone was not sufficient to activate the IFN-γ promoter, activation of both the p38 pathway and NF-κB together induced IFN-γ promoter activity to a level similar to that obtained with RacL61 (Fig. 2D). The JNK pathway does not appear to contribute to IFN-γ promoter activity, because it did not synergize with either NF-κB or p38. Thus, both the p38 and NF-κB pathways are required for Rac-mediated IFN-γ activation, and these two pathways activate the IFN-γ promoter synergistically.

To investigate the role of Rac in T_H1

[1]Section of Immunobiology and [2]Howard Hughes Medical Institute, Yale University School of Medicine, 310 Cedar Street, New Haven, CT 06520–8011, USA. [3]Section of Pediatric Hematology/Oncology, Wells Center for Pediatric Research, Howard Hughes Medical Institute, Indiana University School of Medicine, Indianapolis, IN 46202, USA. [4]Howard Hughes Medical Institute, University of Massachusetts Medical Center, Worcester, MA 01605, USA. [5]Department of Molecular Biophysics and Biochemistry, Yale University School of Medicine, 333 Cedar Street, New Haven, CT 06520–8024, USA.

*Present address: Pfizer, Groton, CT 06340, USA.
†These authors contributed equally to this work.
‡Present address: University of Rochester, Center for Vaccine Biology and Immunology, Post Office Box 609, Rochester, NY 14623, USA.
§Present address: Medizinische Klinik III, Immunologie Labor, Gluckstrabe 41, 91054 Erlangen, Germany.
‖Present address: Lilly Research Laboratory, Eli Lilly and Company, Indianapolis, IN 46285, USA.
¶Present address: The Walter Eliza Hall Institute, Melbourne, Australia.
#To whom correspondence should be addressed: E-mail: fran.manzo@yale.edu